Proinsulin expression shapes the TCR repertoire but fails to control the development of low avidity insulin-reactive CD8$^+$ T cells

James A. Pearson[a], Terri C. Thayer[a], James E. McLaren[b], Kristin Ladell[b], Evy De Leenheer[a], Amy Phillips[a], Joanne Davies[a], Dimitri Kakabadse[a], Kelly Miners[b], Peter Morgan[c], Li Wen[d], David A. Price[b], and F. Susan Wong[a]

[a]Diabetes Research Group, Division of Infection and Immunity, School of Medicine, Cardiff University, Wales, UK

[b]Cellular Immunology Group, Division of Infection and Immunity, School of Medicine, Cardiff University, Wales, UK

[c]Cardiff Business School, Cardiff University, Wales, UK

[d]Section of Endocrinology, School of Medicine, Yale University, New Haven, Connecticut, USA

Correspondence to:

Professor F. S. Wong,
Division of Infection and Immunity,
School of Medicine,
Cardiff University,
Heath Park,
Cardiff CF14 4XN,
Wales, UK.
E-mail: WongFS@cardiff.ac.uk
Phone: +44 029 20687000
Fax: +44 029 20744671

Running title: Proinsulin expression shapes the TCR repertoire

No. of figures: 6
No. of tables: 2
Online appendix data: 3 figures, 2 tables
Word count: 3,832

Abstract

Non-obese diabetic (NOD) mice, a model strain for human type 1 diabetes, express proinsulin (PI) in the thymus. However, insulin-reactive T cells escape negative selection and subsequent activation of the $CD8^+$ T cell clonotype G9C8, which recognizes insulin B15-23 via an αβ T cell receptor (TCR) incorporating *TRAV8-1/TRAJ9* and *TRBV19/TRBJ2-3* gene rearrangements, contributes to the development of diabetes. In this study, we used fixed TRAV8-1/TRAJ9 TCRα chain transgenic mice to assess the impact of PI isoform expression on the insulin-reactive $CD8^+$ T cell repertoire. The key findings were: (i) PI2 deficiency increases the frequency of insulin B15-23-reactive $TRBV19^+CD8^+$ T cells and causes diabetes; (ii) insulin B15-23-reactive $TRBV19^+CD8^+$ T cells are more abundant in the pancreatic lymph nodes of mice lacking PI1 and/or PI2; (iii) overexpression of PI2 decreases TRBV19 usage in the global $CD8^+$ T cell compartment; (iv) a biased repertoire of insulin-reactive $CD8^+$ T cells emerges in the periphery regardless of antigen exposure; and (v) low avidity insulin-reactive $CD8^+$ T cells are less affected by antigen exposure in the thymus compared to the periphery. These findings inform our understanding of the diabetogenic process and potentially reveal new avenues for therapeutic exploitation in type 1 diabetes.

Autoreactive T cells are key players in the process of immune-mediated β cell destruction leading to type I diabetes. Developing $CD4^+CD8^+$ thymocytes that recognize self-derived peptide-major histocompatibility complex (pMHC) molecules via high affinity interactions with a clonotypically expressed T cell receptor (TCR) are typically removed by negative selection to prevent the egress of such autoreactive T cells. Similar deletional processes may also operate in the periphery (1). However, these tolerogenic mechanisms are not infallible, and self-derived antigen-specific T cell escape likely underpins a number of autoimmune diseases.

Proinsulin (PI) is a major diabetogenic autoantigen in humans (2-5) and mice (6-10). It is generated from a larger pre-prohormone by cleavage of the signal peptide, then further processed in the pancreatic β cells to insulin, which is the metabolically active hormone. Self-derived antigens, including PI, are expressed in the thymus (11; 12) under the control of the autoimmune regulator (AIRE) protein, a transcription factor found in medullary thymic epithelial cells (13). Central exposure to these antigens limits the development of autoreactive T cells. Although the MHC locus, encompassing both class I and II genes, is the most important genetic susceptibility factor for type 1 diabetes (14), the insulin 5'-VNTR region also plays a significant role by regulating PI expression in the thymus and pancreas (15). There are two types of PI in mice, known as PI1 and PI2, which are separately encoded in the genome. PI2 is expressed in the thymus and pancreas, whereas PI1 is thought to occur primarily in the pancreas (11; 16), with only low level expression in the thymus (17). For this reason, it has been suggested that PI2 may be more pivotal in the development of T cell tolerance. Investigation of individual PI1 ($PI1^{-/-}$) knockout mice backcrossed to the non-obese diabetic (NOD) background has shown that loss of PI1 reduces the incidence of diabetes (18). In contrast, loss of PI2 in the corresponding $PI2^{-/-}$ model accelerates the development of diabetes in 100% of mice (19). Conversely, thymic overexpression of PI2 on the MHC class

II promoter (NOD*PI2*^{tg}) leads to a decreased incidence of diabetes (20; 21). These findings suggest that PI2 is important for both central and peripheral tolerance.

Insulin-reactive CD4$^+$ and CD8$^+$ T cells have both been shown to be important for the development of diabetes in humans and mice (6-8; 10; 22). The dominant CD8$^+$ T cell epitope in NOD mice, insulin B15-23 (8; 22), overlaps with a longer peptide recognized by diabetogenic CD4$^+$ T cells (23). In a study where both PI1 and PI2 were eliminated, and an altered insulin expressing alanine at position B16 instead of tyrosine was substituted for native insulin, the resulting *PI1*$^{-/-}$*PI2*$^{-/-}$*Y16A*^{tg} mice were protected from diabetes due to removal of the cognate CD4$^+$ and CD8$^+$ autoreactive T cell epitopes (9). However, if both PI1 and PI2 are deleted without insulin substitution, mice die very rapidly from metabolic problems related to insulin deficiency. It is also notable that insulin autoimmunity is required for the development of islet-specific glucose-6-phosphatase catalytic subunit-related protein (IGRP) reactivity (24; 25). Modifying the development of insulin autoimmunity may therefore prove to be a key therapeutic intervention.

We previously generated a highly diabetogenic murine CD8$^+$ T cell clone (G9C8) that expresses an αβ TCR encoded by *TRAV8-1/TRAJ9* and *TRBV19/TRBJ2-3* gene rearrangements (22). *In vitro*, this clone displayed potent cytotoxic and proliferative activity in response to islet cells. *In vivo*, G9C8 caused diabetes within 5-10 days in young pre-diabetic NOD and NOD.*scid* mice (22). Moreover, T cells that recognize the H-2K^d-restricted insulin B15-23 epitope targeted by G9C8 infiltrate the islets of NOD mice at 4 weeks of age, a time when very few T cells with other specificities are present (8; 26). These observations further suggest that CD8$^+$ T cells are important in the pathogenesis of autoimmune diabetes in the NOD mouse model. The insulin B15-23 peptide (LYLVCGERG) binds very poorly to H2-K^d (27; 28). Consequently, relatively high peptide concentrations are required for exogenous recognition of this antigenic complex, which typically elicits low avidity T cells.

Of note, the native B15-23 sequence is conserved in humans, and common to both murine PI1 and PI2.

It is established that $CD8^+$ T cells in humans can recognize antigenic peptides derived from pre-proinsulin and destroy β cells (4; 5). However, the underlying mechanisms that allow the development and expansion of such disease-relevant $CD8^+$ T cell populations remain obscure. In this study, we generated fixed TRAV8-1/TRAJ9 chain NOD mice (designated A22 for simplicity to reflect usage of mouse line 22) (29) with either normal PI1 and PI2 levels (*A22Cα*$^{-/-}$ mice), PI2 overexpression (*A22Cα*$^{-/-}$*PI2*^{tg} mice), PI2 deficiency (*A22Cα*$^{-/-}$*PI2*$^{-/-}$ mice), PI1 deficiency (*A22Cα*$^{-/-}$*PI1*$^{-/-}$mice*),* or both PI1 and PI2 deficiency with a mutant transgene preventing recognition of the insulin B15-23 peptide (*A22Cα*$^{-/-}$*PI1*$^{-/-}$ *PI2*$^{-/-}$*Y16A*^{tg} mice) (Table 1). These unique models were then used to investigate the role of PI expression on the insulin B15-23-reactive $CD8^+$ T cell repertoire.

Research Design and Methods

Mice

Insulin B15-23-reactive TRAV8-1/TRAJ9 TCRα chain transgenic mice were generated as described previously (29). Line 22 was selected for further characterization, hence the designation A22. TCRα chain transgenic mice were crossed with NOD*Cα*$^{-/-}$ mice to generate *A22Cα*$^{-/-}$ mice exclusively expressing the *TRAV8-1/TRAJ9* transgene. These *A22Cα*$^{-/-}$ mice were then crossed with NOD mice overexpressing PI2 under the MHCII promoter (NOD*PI2*^{tg}) to generate *A22Cα*$^{-/-}$*PI2*^{tg} mice. In addition, *A22Cα*$^{-/-}$ mice were crossed with NOD mice lacking PI2, NOD mice lacking PI1, and NOD mice lacking PI1 and PI2 but reconstituted with a mutant transgene encoding a tyrosine-to-alanine mutation at position 16 of the insulin B chain (9) to generate *A22Cα*$^{-/-}$*PI2*$^{-/-}$ mice, *A22Cα*$^{-/-}$*PI1*$^{-/-}$ mice, and *A22Cα*$^{-/-}$ *PI1*$^{-/-}$*PI2*$^{-/-}$*Y16A*^{tg} mice, respectively (Table 1). Mice were housed in microisolators or scantainers in the specific pathogen-free facility at Cardiff University. All procedures were performed in accordance with protocols approved by the UK Home Office.

Flow cytometric analysis of TCRVβ expression

Thymus, spleen, pancreatic lymph nodes (PLN), and mesenteric lymph nodes (MLN) were harvested from mice aged 4-7 weeks, 8-10 weeks, and 12-16 weeks. Single cell suspensions were generated and stained with mAbs specific for CD4, CD8α, CD19, and 14 distinct TCRVβ chains (2-14 and 17). Live single CD8^{+} T cells were then gated to visualize TCRVβ expression patterns. Data were analyzed with FlowJo software version 7.6.5 (Treestar Inc.).

Tetramer analysis

Thymus, spleen, PLN, and MLN were harvested from TCRα transgenic mice and polyclonal NOD mice at 4-8 weeks of age. Single cell suspensions were generated and stained serially with pre-titrated concentrations of the H-2K^{d}-LYLVCGERG tetramer (National Institutes of

Health Tetramer Core Facility), a viability dye, and the following mAbs: αCD4-PECy7, αCD8α-FITC, αCD11b-APC, and αCD19-PerCPCy5.5. Data were analyzed with FlowJo software version 7.6.5 (Treestar Inc.). T cells from G9C8 transgenic mice (29) were used as a positive control. The minimal H-2K^{d}-AYAAAAAAV tetramer was used to determine non-specific background.

TRBV19^{+}CD8^{+} T cell isolation and expansion

Single cell PLN suspensions from 6-week-old *A22Cα*$^{-/-}$ mice, *A22Cα*$^{-/-}$*PI2*$^{-/-}$ mice, and *A22Cα*$^{-/-}$*PI1*$^{-/-}$*PI2*$^{-/-}$*Y16A*^{tg} mice were sorted by flow cytometry for live CD4^{-}CD8^{+}CD11b^{-}CD19^{-}TCRVβ6^{+} events. Cells were initially cultured in bulk with the addition of IL-2 (20U/ml), IL-7 (2ng/ml), and insulin B15-23 peptide (1μg/ml) in RPMI complete medium (2mM L-glutamine, 100U/ml penicillin, 0.1mg/ml streptomycin, 5% fetal bovine serum, and 0.05mM 2-mercaptoethanol in RPMI 1640). Expanding cells were re-plated after limiting dilution and grown to sufficient numbers for functional analysis.

Cytotoxicity assays

Expanded TRBV19^{+}CD8^{+} T cells were washed twice in RPMI complete medium to remove cytokines from the culture. P815 cells (targets) were labeled with PKH-26 (Sigma) and incubated with TRBV19^{+}CD8^{+} T cells (effectors) in the presence of insulin B15-23 peptide at an effector-to-target (E:T) ratio of 10:1 for 16 hours at 37°C. TOPRO-3 iodide was added immediately prior to flow cytometric analysis. Single PKH-26^{+}TOPRO-3^{+} P815 cells were gated, and cytotoxicity was expressed as the percentage of dead cells/total targets (30). Specific target cell killing was corrected for spontaneous background death by subtracting the percentage of dead cells in the control sample comprising targets with T cells in the absence of peptide.

Enzyme-linked immunosorbent assays

TRBV19^{+}CD8^{+} T cells were co-cultured with irradiated bone marrow-derived dendritic cells in the presence of insulin B15-23 peptide at an E:T ratio of 10:1 for 48 hours at 37°C. Supernatants were analyzed for MIP1β and IFNγ levels according to the manufacturer's instructions (R&D Systems and eBioscience, respectively).

TCR clonotyping

Clonotypic analysis of H-2K^{d}-LYLVCGERG tetramer^{+}CD8^{+} T cells and oligoclonal lines was performed as described previously with minor modifications (31). Briefly, viable tetramer^{+}CD8^{+} T cells (n=43-2,353) from individual mice or TRBV19^{+}CD8^{+} T cells (n=5,000) from individual oligoclonal lines were sorted directly into 1.5ml microtubes (Sarstedt) containing 100μl RNAlater (Applied Biosystems) using a custom-modified FACS Aria II flow cytometer (BD Biosciences). Unbiased amplification of all expressed *TRBV* gene products was conducted using a template-switch anchored RT-PCR with a 3' constant region primer (5'-TGGCTCAAACAAGGAGACCT-3'). Amplicons were sub-cloned, sampled, sequenced, and analyzed as described previously (32). Concatenated data are shown for each genetic strain. The IMGT nomenclature is used in this report (33).

Histology

Immunohistochemistry was performed on fixed pancreata as described previously (29). Sections were scored for insulitis after staining with hematoxylin and eosin (Vector Laboratories).

Statistics

Statistical analyses were conducted using ANOVA tests or Student's t-test with R software. Bonferroni correction was used for multiple comparisons such that $p<0.05$ is equivalent to $p<0.0000022907$ and $p<0.01$ is equivalent to $p<0.0000004581$.

Results

$CD4^+$ and $CD8^+$ T cell numbers are not affected by PI expression

In preliminary experiments, we used flow cytometry to assess the impact of PI expression on T cell lineage development in our mouse models (*A22Cα*$^{-/-}$, *A22Cα*$^{-/-}$*PI2*^{tg}, *A22Cα*$^{-/-}$*PI2*$^{-/-}$, *A22Cα*$^{-/-}$*PI1*$^{-/-}$, and *A22Cα*$^{-/-}$*PI1*$^{-/-}$*PI2*$^{-/-}$*Y16A*^{tg}). Groups of mice were screened at 4-7 weeks and 12-16 weeks. No significant differences in $CD4^+$ or $CD8^+$ T cell numbers were apparent between strains regardless of age, either in the thymus (Figure 1) or in the periphery (Supplemental Figure 1). However, a substantial reduction in the total number of $CD4^+$ T cells was observed for all TCRα chain transgenic strains relative to polyclonal NOD mice (Figure 1 and Supplemental Figure 1).

PI expression alters the proportion of $TRBV19^+CD8^+$ T cells

To evaluate the global influence of PI expression on the $CD8^+$ T cell repertoire, 14 TCRVβ-specific mAbs were used to assess TRBV usage by $CD8^+$ T cells isolated from the thymus, spleen, and lymph nodes of the different *A22Cα*$^{-/-}$ mice aged either 4-7 weeks or 12-16 weeks. A strong PI-mediated effect was observed on the expression of TRBV19 (Vβ6), which encodes the TCRVβ chain used by the G9C8 clone (Figure 2 and Supplemental Figure 2). Specifically, the proportion of $TRBV19^+CD8^+$ T cells, both in the thymus and the periphery, decreased with age in *A22Cα*$^{-/-}$ mice (Figure 2). This effect was more pronounced in mice with PI2 overexpression (*A22Cα*$^{-/-}$*PI2*^{tg}), which also displayed lower proportions of $TRBV19^+CD8^+$ T cells compared to *A22Cα*$^{-/-}$ mice, notably approximating those observed in polyclonal NOD mice. However, mice lacking PI1 (*A22Cα*$^{-/-}$*PI1*$^{-/-}$), PI2 (*A22Cα*$^{-/-}$*PI2*$^{-/-}$), or both PI genes (*A22Cα*$^{-/-}$*PI1*$^{-/-}$*PI2*$^{-/-}$*Y16A*^{tg}) showed no significant changes in the proportion of $TRBV19^+CD8^+$ T cells with age. Similar trends were observed with respect to the absolute number of $TRBV19^+CD8^+$ T cells, which declined with age but differed between strains only

in PLN at 12-16 weeks, where a substantial reduction was observed in *A22Cα*$^{-/-}$*PI2*^{tg} mice (Supplemental Figure 2). Less marked effects were noted with other TRBV segments. In particular, the proportion of CD8^{+} T cells expressing TRBV13 (Vβ8), the most commonly employed gene segment in NOD mice, was unaffected by proinsulin expression (data not shown).

Insulin B15-23-reactive CD8^{+} T cells are increased in mice lacking PI1 or PI2

As the TRAV8-1/TRAJ9 chain used by these mice specifically recognizes the insulin B15-23 epitope, we used H-2K^{d}-LYLVCGERG tetramers to quantify the effect of PI expression on the development of insulin B15-23-reactive CD8^{+} T cells (Supplemental Figure 3A). Increased numbers and percentages of tetramer^{+}CD8^{+} T cells were detected in the thymus, spleen, and PLN of PI2 deficient (*A22Cα*$^{-/-}$*PI2*$^{-/-}$) mice compared to wildtype *A22Cα*$^{-/-}$ mice (Figure 3 and Supplemental Figure 3). Interestingly, *A22Cα*$^{-/-}$*PI1*$^{-/-}$ mice also showed an increased proportion of insulin B15-23-reactive CD8^{+} T cells in PLN compared to *A22Cα*$^{-/-}$ mice, whereas a smaller increase was observed in PLN from *A22Cα*$^{-/-}$*PI1*$^{-/-}$*PI2*$^{-/-}$*Y16A*^{tg} mice despite greater enhancements in the thymus and spleen. However, only the *A22Cα*$^{-/-}$*PI2*$^{-/-}$ and *A22Cα*$^{-/-}$*PI1*$^{-/-}$*PI2*$^{-/-}$*Y16A*^{tg} strains exhibited an increase in the number of insulin B15-23-reactive CD8^{+} T cells in both the thymus and the periphery (Supplemental Figure 3B). It is also notable that no differences in tetramer staining intensity were detected between strains, indicating equivalent levels of cognate TCR expression (Supplemental Figure 3C).

Insulin B15-23-reactive CD8^{+} T cells cause spontaneous diabetes in PI2 deficient mice

To assess the biological relevance of these proportional and numerical differences in insulin B15-23-reactive CD8^{+} T cells, we examined the incidence of spontaneous diabetes across strains. Strikingly, diabetes occurred spontaneously only in male PI2 deficient (*A22Cα*$^{-/-}$*PI2*$^{-/-}$) mice (Figure 4). Moreover, disease onset was considerably accelerated in this group

compared to male wildtype NOD mice, which develop diabetes after 20 weeks of age in our colony with a final incidence of 20% by 35 weeks (data not shown). Mild insulitis was detected in male *A22Cα*$^{-/-}$ and non-diabetic *A22Cα*$^{-/-}$*PI2*$^{-/-}$ mice, while normal pancreatic histology was observed in male *A22Cα*$^{-/-}$*PI1*$^{-/-}$*PI2*$^{-/-}$*Y16A*^{tg} mice (Supplemental Table 1). These findings suggest that PI2 deficiency permits the development of diabetogenic insulin B15-23-reactive CD8^{+} T cells.

Insulin B15-23-reactive CD8^{+} T cells express multiple TRBV chains and exhibit PI-specific changes in TRBV19 usage

To further our understanding of the diabetogenic process, we evaluated the TCR repertoire specifically within the insulin B15-23-reactive CD8^{+} T cell population. Data are shown for wildtype mice (*A22Cα*$^{-/-}$), PI2 overexpressing mice (*A22Cα*$^{-/-}$*PI2*^{tg}), PI2 deficient mice (*A22Cα*$^{-/-}$*PI2*$^{-/-}$), and mice lacking both PI1 and PI2 (*A22Cα*$^{-/-}$*PI1*$^{-/-}$*PI2*$^{-/-}$*Y16A*^{tg}). By sequencing expressed *TRB* transcripts in H-2K^{d}-LYLVCGERG tetramer^{+}CD8^{+} T cells from PLN, we identified a restricted TCR repertoire in all four groups of mice (Figure 5). Alterations in PI expression clearly influenced *TRBV* gene selection in insulin B15-23-reactive CD8^{+} T cells. Most notably, the proportion of TRBV19^{+}CD8^{+} T cells increased when PI2 or both PI1 and PI2 were absent. Moreover, no TRBV19 sequences were detected when PI2 was overexpressed. These observations suggest that PI expression critically affects the selection of insulin B15-23-reactive TCRs, even in the context of a highly restricted clonotypic repertoire.

Insulin B15-23-reactive TRBV19^{+}CD8^{+} T cells exhibit low functional sensitivity irrespective of PI expression during development

As the selection of insulin B15-23-reactive TRBV19^{+}CD8^{+} T cells was influenced by PI expression, we next investigated the role of antigen exposure as a determinant of cellular function. TRBV19^{+}CD8^{+} T cells from wildtype (*A22Cα*$^{-/-}$), PI2 deficient (*A22Cα*$^{-/-}$*PI2*$^{-/-}$), or

PI1 and PI2 deficient (*A22Cα*$^{-/-}$*PI1*$^{-/-}$*PI2*$^{-/-}$*Y16A*^{tg}) mice were isolated and cultured briefly with the cognate peptide in the presence of IL-2 and IL-7 to generate a panel of insulin B15-23-reactive oligoclonal T cell lines. The functional profile of these lines was assayed by measuring cytotoxicity and proinflammatory cytokine (MIP1β and IFNγ) production in response to the insulin B15-23 peptide. Similar cytotoxic responses were observed for all strains regardless of PI expression, and target cell lysis required high doses of exogenous peptide (Figure 6A). Lines generated from *A22Cα*$^{-/-}$*PI1*$^{-/-}$*PI2*$^{-/-}$*Y16A*^{tg} mice displayed enhanced MIP1β responses (Figure 6B) but produced less IFNγ compared to wildtype (Figure 6C). Overall, these results suggest that insulin B15-23-reactive TRBV19^{+}CD8^{+} T cells exhibit intrinsically low levels of functional sensitivity and that altered reactivity to cognate antigen does not underlie the development of spontaneous diabetes in PI2 deficient (*A22Cα*$^{-/-}$*PI2*$^{-/-}$) mice.

Insulin B15-23-reactive TRBV19^{+}CD8^{+} T cells use TRBJ2-3 and exhibit a common TCR CDR3β motif

The highly diabetogenic G9C8 clone expresses a *TRBV19/TRBJ2-3* gene-encoded TCRβ chain (22). Although no obvious differences in functional sensitivity were observed between insulin B15-23-reactive CD8^{+} T cell clonotypes selected in mice with differing levels of PI expression, we nonetheless conducted a molecular analysis of *TRB* gene rearrangements in our oligoclonal antigen-specific lines to see if PI expression impinges on TCR selection. All lines were dominated by TRBV19^{+} TCRs, and 9 of the 20 were monoclonal. We obtained 11 unique TRBV19-associated CDR3β sequences, 5 of which were private and 6 of which were shared (Table 2). Ten of these distinct CDR3β sequences incorporated TRBJ2-3 with a fixed loop length of 13 amino acids generating a motif (CASS-XXXX-GAETLY) in common with the original G9C8 clone (CASS-IRDR-GAETLY). Moreover, arginine was universally conserved at position 6 in these CDR3β sequences, likely providing an important contact

residue for recognition of the insulin B15-23 peptide. Non-polar side chain amino acids were preferred at position 5 (with the exception of arginine), whereas amino acids with acidic side chains (aspartic acid or glutamic acid) or uncharged polar side chains (glutamine or threonine) were preferred at position 7. Little preference was observed for any particular residue at position 8. In contrast, we found very limited sequence similarity across the CDR3β loop within the tetramer^{+}CD8^{+} T cell population as a whole (Figure 3). One common CDR3β sequence (CASSLGGYEQY) was found in *A22Cα*$^{-/-}$ and *A22Cα*$^{-/-}$*PI2*$^{-/-}$ mice, and another (CASSRVPGEQY) was found in more than one *A22Cα*$^{-/-}$ mouse (Supplemental Table 2). We also examined sequences of TRBV19+ non-insulin B15-23 reactive T cells in each of the 4 strains of transgenic mice. We noted that the TRBJ2-3 incorporated motif (CASS-XXXX-GAETLY) was not found in these T cells (data not shown). Collectively, these data demonstrate that insulin B15-23 elicits a highly biased TRBV19^{+} repertoire consistent with a strict docking mode for TCR recognition dictated by structural constraints.

Discussion

In this paper, we report five principal findings based on an in-depth analysis of fixed TCRα chain NOD mice. First, PI1 or PI2 deficiency is associated with peripheral expansion and significant increases in insulin B15-23-reactive $CD8^+$ T cells in the draining lymph node for the pancreas, the target organ in type 1 diabetes. Second, the proportion of insulin B15-23-reactive $CD8^+$ T cells expressing TRBV19 increases in the absence of PI. This repertoire shift potentially contributes to the development of autoimmune diabetes. Third, variations in PI expression alter global *TRBV* gene usage in the $CD8^+$ T cell compartment. In particular, $TRBV19^+CD8^+$ T cell numbers were reduced significantly upon increased exposure to PI2 through transgenic overexpression, although deletion of either the PI1 or PI2 genes alone did not change the frequency of this population. Fourth, insulin B15-23-reactive $TRBV19^+CD8^+$ T cells display low levels of functional sensitivity for the cognate peptide irrespective of PI expression, consistent with a lack of epitope-regulated negative selection in the thymus. Fifth, antigen recognition by insulin B15-23-reactive $TRBV19^+CD8^+$ T cells is driven by a highly biased set of TCRs characterized by *TRBJ2-3* gene usage and the presence of a conserved non-germline-encoded arginine residue at position 6 in the CDR3β loop. To our knowledge, this is the first demonstration that proinsulin expression can directly affect the development of autoreactive TCRs.

PI2 is expressed in the thymus and has been shown to promote tolerance (17; 20; 21; 34). As a consequence, NOD mice with PI2 deficiency develop accelerated diabetes (19). However, NOD mice lacking PI1 do not develop autoimmune diabetes, presumably because PI2 tolerizes potentially autoreactive T cells (18). Although both PI1 and PI2 are expressed in the thymus, PI2 is the predominant isoform; equivalent levels of PI1 and PI2 are found in the periphery (17; 35; 36). It is notable in this regard that PI deficiency enhanced the development of $TRBV19^+CD8^+$ T cells in the thymus and minimized corresponding age-

related declines in the periphery. These data suggest that both PI1 and PI2 have tolerogenic properties, with the weak effects on disease likely related to the low frequency of insulin B15-23-reactive cells in the overall TRBV19^{+}CD8^{+} T cell population.

Antigen encounter in the thymus preferentially deletes high avidity T cells (37; 38). Consistent with this process, our data show that increased numbers of insulin B15-23-reactive CD8^{+} T cells are present in mice lacking either PI2 alone or both PI1 and PI2, probably due to a lack of negative selection. Moreover, only PI2 deficient mice developed diabetes in our study. It is remarkable that male mice were exclusively affected in this regard, despite equivalent increases in insulin-reactive CD8^{+} T cells in female mice lacking PI2. Recent data suggest that non-immune factors, including interactions between gut microbiota and androgens (39; 40), may contribute to such sexual dimorphism in the development of diabetes. Irrespective of the underlying mechanism, however, these findings suggest that insulin B15-23-reactive CD8^{+} T cells are important determinants of disease because *A22Cα*$^{-/-}$ *PI1*$^{-/-}$*PI2*$^{-/-}$*Y16A*^{tg} mice express a mutant transgene that prevents recognition of the cognate peptide.

It is notable that we did not detect any significant functional differences in insulin B15-23-reactive TRBV19^{+}CD8^{+} T cells across strains of mice with altered levels of PI expression. This counterintuitive finding may reflect *in vitro* activation and expansion prior to assay, which could mask intrinsic differences in the *ex vivo* setting, or a convergence of functional properties due to the expression of PI in peripheral lymphoid tissue (13; 41). Regardless of origin, these autoreactive cells expressed very similar TRBV19/TRBJ2-3 transcripts incorporating a CDR3β motif based around a central arginine residue. Arginine is degenerately encoded at the nucleotide level and readily incorporated on a probabilistic basis during the somatic recombination process (42). It can also play a key role in TCR recognition

(43). Our data therefore suggest a highly conserved mode of antigen engagement focused on the G9C8 'blueprint'.

Several studies have previously identified a tolerogenic role for PI2 (17; 19; 20; 21). In contrast, the role of PI1 has not been fully established. The only reported investigation in NOD mice found that PI1 deficiency protected against the development of diabetes (18). Interestingly, on a non-autoimmune background (129/SV), mice lacking PI2 showed increased PI1 gene transcripts as well as enhanced β cell mass to compensate for lower insulin production, indicating the importance of PI1 in metabolism (44). Moreover, the PI2 B9-23 peptide can induce proliferation of PI1-reactive NOD T cells, and both the PI1 B9-23 and C49-66 peptides can induce proliferation of PI2-reactive NOD T cells (21). Such cross-reactivity suggests that both isoforms can facilitate the expansion of PI-specific populations in the periphery. Further studies are therefore required to assess the relative contributions of PI1 and PI2 as determinants of tolerance and diabetogenicity.

Although our model system addresses a single specificity, the epitope nonetheless derives from insulin, which is known to be an important early antigenic target in type 1 diabetes. Previous work by other investigators has focused on IGRP-specific NY8.3 $CD8^+$ T cells (45-47). However, there are fundamental differences between these two diabetogenic epitopes. Most notably, IGRP is not expressed in the thymus (1). In contrast, studies of proinsulin facilitate an understanding of repertoire development in the presence of an autoantigen that is naturally expressed in the thymus and the periphery. Moreover, IGRP reactivity is dependent on an autoimmune response to insulin (24; 25). In humans, the key genetic susceptibility region IDDM2 relates to the level of proinsulin expression. Our study is therefore informative because it describes the impact of variable proinsulin expression on clonotype selection in response to a defined and biologically relevant autoimmune epitope in type 1 diabetes.

Two important conclusions emerge from the present data. First, proinsulin expression shapes the insulin-reactive $CD8^+$ T cell repertoire in a mouse model of type 1 diabetes. Second, an avidity threshold exists below which insulin-reactive $CD8^+$ T cells are less affected by antigen exposure in the thymus compared to the periphery. These findings have potential implications for the induction of antigen-specific tolerance as a therapeutic strategy against autoimmune diabetes.

Acknowledgements

We thank the National Institutes of Health Tetramer Core Facility for provision of the H-2K^{d}-LYLVCGERG tetramer and various control tetramers. Profs L.C. Harrison and A. Lew (Walter and Eliza Hall Research Institute, Melbourne, Australia) kindly provided NOD mice overexpressing PI2 (NOD*PI2*^{tg}) under the MHCII promoter before they were available commercially.

Author Contributions

J.A.P., T.C.T., J.E.M., K.L., E.D.L., A.P., J.D., D.K., and K.M. carried out experiments; J.A.P., J.E.M., P.M., L.W., D.A.P., and F.S.W. analyzed data; P.M. assisted with statistical analysis; J.A.P., D.A.P., and F.S.W. wrote the manuscript; J.A.P., T.C.T., J.E.M., K.L., L.W., D.A.P., and F.S.W. edited the manuscript. The project was conceived by F.S.W., who assumes responsibility for the work.

Funding

This work was supported by the Medical Research Council (grant G0901155) and the Wellcome Trust (grant 100326Z/12/Z). J.A.P. was the recipient of a Diabetes UK Studentship (08/3767). D.A.P. is a Wellcome Trust Senior Investigator.

Author Disclosures

There are no competing financial conflicts of interest.

Prior Presentation

Parts of this study were presented in abstract form at the Immunology of Diabetes Conference (2013), the Diabetes UK Annual Professional Conference (2013 and 2014), and the British Society for Immunology Conference (2014).

References

1. Gardner JM, Devoss JJ, Friedman RS, Wong DJ, Tan YX, Zhou X, Johannes KP, Su MA, Chang HY, Krummel MF, Anderson MS: Deletional tolerance mediated by extrathymic Aire-expressing cells. Science 2008;321:843-847
2. Schloot NC, Willemen S, Duinkerken G, de Vries RR, Roep BO: Cloned T cells from a recent onset IDDM patient reactive with insulin B-chain. J Autoimmun 1998;11:169-175
3. Semana G, Gausling R, Jackson RA, Hafler DA: T cell autoreactivity to proinsulin epitopes in diabetic patients and healthy subjects. J Autoimmun 1999;12:259-267
4. Skowera A, Ellis RJ, Varela-Calviño R, Arif S, Huang GC, Van-Krinks C, Zaremba A, Rackham C, Allen JS, Tree TI, Zhao M, Dayan CM, Sewell AK, Unger WW, Unger W, Drijfhout JW, Ossendorp F, Roep BO, Peakman M: CTLs are targeted to kill beta cells in patients with type 1 diabetes through recognition of a glucose-regulated preproinsulin epitope. J Clin Invest 2008;118:3390-3402
5. Bulek AM, Cole DK, Skowera A, Dolton G, Gras S, Madura F, Fuller A, Miles JJ, Gostick E, Price DA, Drijfhout JW, Knight RR, Huang GC, Lissin N, Molloy PE, Wooldridge L, Jakobsen BK, Rossjohn J, Peakman M, Rizkallah PJ, Sewell AK: Structural basis for the killing of human beta cells by CD8(+) T cells in type 1 diabetes. Nat Immunol 2012;13:283-289
6. Wegmann DR, Gill RG, Norbury-Glaser M, Schloot N, Daniel D: Analysis of the spontaneous T cell response to insulin in NOD mice. J Autoimmun 1994;7:833-843
7. Zekzer D, Wong FS, Wen L, Altieri M, Gurlo T, von Grafenstein H, Sherwin RS: Inhibition of diabetes by an insulin-reactive CD4 T-cell clone in the nonobese diabetic mouse. Diabetes 1997;46:1124-1132
8. Wong FS, Karttunen J, Dumont C, Wen L, Visintin I, Pilip IM, Shastri N, Pamer EG, Janeway CA: Identification of an MHC class I-restricted autoantigen in type 1 diabetes by screening an organ-specific cDNA library. Nat Med 1999;5:1026-1031
9. Nakayama M, Abiru N, Moriyama H, Babaya N, Liu E, Miao D, Yu L, Wegmann DR, Hutton JC, Elliott JF, Eisenbarth GS: Prime role for an insulin epitope in the development of type 1 diabetes in NOD mice. Nature 2005;435:220-223
10. Lamont D, Mukherjee G, Kumar PR, Samanta D, McPhee CG, Kay TW, Almo SC, DiLorenzo TP, Serreze DV: Compensatory mechanisms allow undersized anchor-deficient class I MHC ligands to mediate pathogenic autoreactive T cell responses. J Immunol 2014;193:2135-2146
11. Derbinski J, Schulte A, Kyewski B, Klein L: Promiscuous gene expression in medullary thymic epithelial cells mirrors the peripheral self. Nat Immunol 2001;2:1032-1039
12. Pugliese A, Zeller M, Fernandez A, Jr., Zalcberg LJ, Bartlett RJ, Ricordi C, Pietropaolo M, Eisenbarth GS, Bennett ST, Patel DD: The insulin gene is transcribed in the human thymus and transcription levels correlated with allelic variation at the INS VNTR-IDDM2 susceptibility locus for type 1 diabetes. Nat Genet 1997;15:293-297
13. Anderson MS, Venanzi ES, Klein L, Chen Z, Berzins SP, Turley SJ, von Boehmer H, Bronson R, Dierich A, Benoist C, Mathis D: Projection of an immunological self shadow within the thymus by the aire protein. Science 2002;298:1395-1401
14. Nejentsev S, Howson JM, Walker NM, Szeszko J, Field SF, Stevens HE, Reynolds P, Hardy M, King E, Masters J, Hulme J, Maier LM, Smyth D, Bailey R, Cooper JD, Ribas G, Campbell RD, Clayton DG, Todd JA, Consortium WTCC: Localization of type 1 diabetes susceptibility to the MHC class I genes HLA-B and HLA-A. Nature 2007;450:887-892
15. Vafiadis P, Bennett ST, Todd JA, Nadeau J, Grabs R, Goodyer CG, Wickramasinghe S, Colle E, Polychronakos C: Insulin expression in human thymus is modulated by INS VNTR alleles at the IDDM2 locus. Nat Genet 1997;15:289-292
16. Deltour L, Leduque P, Blume N, Madsen O, Dubois P, Jami J, Bucchini D: Differential expression of the two nonallelic proinsulin genes in the developing mouse embryo. Proc Natl Acad Sci U S A 1993;90:527-531
17. Chentoufi AA, Polychronakos C: Insulin expression levels in the thymus modulate insulin-specific autoreactive T-cell tolerance: the mechanism by which the IDDM2 locus may predispose to diabetes. Diabetes 2002;51:1383-1390

18. Moriyama H, Abiru N, Paronen J, Sikora K, Liu E, Miao D, Devendra D, Beilke J, Gianani R, Gill RG, Eisenbarth GS: Evidence for a primary islet autoantigen (preproinsulin 1) for insulitis and diabetes in the nonobese diabetic mouse. Proc Natl Acad Sci U S A 2003;100:10376-10381
19. Thebault-Baumont K, Dubois-Laforgue D, Krief P, Briand JP, Halbout P, Vallon-Geoffroy K, Morin J, Laloux V, Lehuen A, Carel JC, Jami J, Muller S, Boitard C: Acceleration of type 1 diabetes mellitus in proinsulin 2-deficient NOD mice. J Clin Invest 2003;111:851-857
20. French MB, Allison J, Cram DS, Thomas HE, Dempsey-Collier M, Silva A, Georgiou HM, Kay TW, Harrison LC, Lew AM: Transgenic expression of mouse proinsulin II prevents diabetes in nonobese diabetic mice. Diabetes 1997;46:34-39
21. Jaeckel E, Lipes MA, von Boehmer H: Recessive tolerance to preproinsulin 2 reduces but does not abolish type 1 diabetes. Nat Immunol 2004;5:1028-1035
22. Wong FS, Visintin I, Wen L, Flavell RA, Janeway CA: CD8 T cell clones from young nonobese diabetic (NOD) islets can transfer rapid onset of diabetes in NOD mice in the absence of CD4 cells. J Exp Med 1996;183:67-76
23. Daniel D, Wegmann DR: Protection of nonobese diabetic mice from diabetes by intranasal or subcutaneous administration of insulin peptide B-(9-23). Proc Natl Acad Sci U S A 1996;93:956-960
24. Krishnamurthy B, Dudek NL, McKenzie MD, Purcell AW, Brooks AG, Gellert S, Colman PG, Harrison LC, Lew AM, Thomas HE, Kay TW: Responses against islet antigens in NOD mice are prevented by tolerance to proinsulin but not IGRP. J Clin Invest 2006;116:3258-3265
25. Krishnamurthy B, Mariana L, Gellert SA, Colman PG, Harrison LC, Lew AM, Santamaria P, Thomas HE, Kay TW: Autoimmunity to both proinsulin and IGRP is required for diabetes in nonobese diabetic 8.3 TCR transgenic mice. J Immunol 2008;180:4458-4464
26. Trudeau JD, Kelly-Smith C, Verchere CB, Elliott JF, Dutz JP, Finegood DT, Santamaria P, Tan R: Prediction of spontaneous autoimmune diabetes in NOD mice by quantification of autoreactive T cells in peripheral blood. J Clin Invest 2003;111:217-223
27. Wong FS, Moustakas AK, Wen L, Papadopoulos GK, Janeway CA, Jr.: Analysis of structure and function relationships of an autoantigenic peptide of insulin bound to H-2K(d) that stimulates CD8 T cells in insulin-dependent diabetes mellitus. Proc Natl Acad Sci U S A 2002;99:5551-5556.
28. Motozono C, Pearson JA, De Leenheer E, Rizkallah PJ, Beck K, Trimby A, Sewell AK, Wong FS, Cole DK: Distortion of the MHC class I binding groove to accommodate an insulin-derived 10-mer peptide. J Biol Chem 2015;290:18924-18933
29. Wong FS, Siew LK, Scott G, Thomas IJ, Chapman S, Viret C, Wen L: Activation of insulin-reactive CD8 T-cells for development of autoimmune diabetes. Diabetes 2009;58:1156-1164
30. Scott GS, Fishman S, Khai Siew L, Margalit A, Chapman S, Chervonsky AV, Wen L, Gross G, Wong FS: Immunotargeting of insulin reactive CD8 T cells to prevent diabetes. J Autoimmun 2010;35:390-397
31. Quigley MF, Almeida JR, Price DA, Douek DC: Unbiased molecular analysis of T cell receptor expression using template-switch anchored RT-PCR. Curr Protoc Immunol 2011;Chapter 10:Unit10.33
32. Price DA, Brenchley JM, Ruff LE, Betts MR, Hill BJ, Roederer M, Koup RA, Migueles SA, Gostick E, Wooldridge L, Sewell AK, Connors M, Douek DC: Avidity for antigen shapes clonal dominance in CD8+ T cell populations specific for persistent DNA viruses. J Exp Med 2005;202:1349-1361
33. Lefranc MP, Pommié C, Ruiz M, Giudicelli V, Foulquier E, Truong L, Thouvenin-Contet V, Lefranc G: IMGT unique numbering for immunoglobulin and T cell receptor variable domains and Ig superfamily V-like domains. Dev Comp Immunol 2003;27:55-77
34. Faideau B, Briand JP, Lotton C, Tardivel I, Halbout P, Jami J, Elliott JF, Krief P, Muller S, Boitard C, Carel JC: Expression of preproinsulin-2 gene shapes the immune response to preproinsulin in normal mice. J Immunol 2004;172:25-33
35. Chentoufi AA, Palumbo M, Polychronakos C: Proinsulin expression by Hassall's corpuscles in the mouse thymus. Diabetes 2004;53:354-359
36. Palumbo MO, Levi D, Chentoufi AA, Polychronakos C: Isolation and characterization of proinsulin-producing medullary thymic epithelial cell clones. Diabetes 2006;55:2595-2601
37. Zehn D, Bevan MJ: T cells with low avidity for a tissue-restricted antigen routinely evade central and peripheral tolerance and cause autoimmunity. Immunity 2006;25:261-270

38. Enouz S, Carrié L, Merkler D, Bevan MJ, Zehn D: Autoreactive T cells bypass negative selection and respond to self-antigen stimulation during infection. J Exp Med 2012;209:1769-1779
39. Markle JG, Frank DN, Mortin-Toth S, Robertson CE, Feazel LM, Rolle-Kampczyk U, von Bergen M, McCoy KD, Macpherson AJ, Danska JS: Sex differences in the gut microbiome drive hormone-dependent regulation of autoimmunity. Science 2013;339:1084-1088
40. Yurkovetskiy L, Burrows M, Khan AA, Graham L, Volchkov P, Becker L, Antonopoulos D, Umesaki Y, Chervonsky AV: Gender bias in autoimmunity is influenced by microbiota. Immunity 2013;39:400-412
41. Lee JW, Epardaud M, Sun J, Becker JE, Cheng AC, Yonekura AR, Heath JK, Turley SJ: Peripheral antigen display by lymph node stroma promotes T cell tolerance to intestinal self. Nat Immunol 2007;8:181-190
42. Venturi V, Price DA, Douek DC, Davenport MP: The molecular basis for public T-cell responses? Nat Rev Immunol 2008;8:231-238
43. Stewart-Jones GB, McMichael AJ, Bell JI, Stuart DI, Jones EY: A structural basis for immunodominant human T cell receptor recognition. Nat Immunol 2003;4:657-663
44. Leroux L, Desbois P, Lamotte L, Duvillié B, Cordonnier N, Jackerott M, Jami J, Bucchini D, Joshi RL: Compensatory responses in mice carrying a null mutation for Ins1 or Ins2. Diabetes 2001;50 Suppl 1:S150-153
45. Verdaguer J, Yoon JW, Anderson B, Averill N, Utsugi T, Park BJ, Santamaria P: Acceleration of spontaneous diabetes in TCR-beta-transgenic nonobese diabetic mice by beta-cell cytotoxic CD8+ T cells expressing identical endogenous TCR-alpha chains. J Immunol 1996;157:4726-4735
46. Amrani A, Verdaguer J, Serra P, Tafuro S, Tan R, Santamaria P: Progression of autoimmune diabetes driven by avidity maturation of a T-cell population. Nature 2000;406:739-742
47. Lieberman SM, Evans AM, Han B, Takaki T, Vinnitskaya Y, Caldwell JA, Serreze DV, Shabanowitz J, Hunt DF, Nathenson SG, Santamaria P, DiLorenzo TP: Identification of the beta cell antigen targeted by a prevalent population of pathogenic CD8+ T cells in autoimmune diabetes. Proc Natl Acad Sci U S A 2003;100:8384-8388

Genotype	TCRα chain	TCRβ chain	Proinsulin 1 expression	Proinsulin 2 expression	Diabetes
A22Cα$^{-/-}$	G9 TCRα transgene (insulin B15-23-specific)	Endogenous TCRβ chains	Normal	Normal	No diabetes
A22Cα$^{-/-}$*PI2*^{tg}	G9 TCRα transgene (insulin B15-23-specific)	Endogenous TCRβ chains	Normal	Overexpression (under MHCII promoter)	No diabetes
A22Cα$^{-/-}$*PI1*$^{-/-}$	G9 TCRα transgene (insulin B15-23-specific)	Endogenous TCRβ chains	Deficient	Normal	No diabetes
A22Cα$^{-/-}$*PI2*$^{-/-}$	G9 TCRα transgene (insulin B15-23-specific)	Endogenous TCRβ chains	Normal	Deficient	Accelerated diabetes in males
A22Cα$^{-/-}$*PI1*$^{-/-}$ *PI2*$^{-/-}$*Y16A*^{tg}	G9 TCRα transgene (insulin B15-23-specific)	Endogenous TCRβ chains	Lack both native proinsulin genes but express a mutated insulin transgene		No diabetes

Table 1: Transgenic and knockout mice used in this study.

DONOR STRAIN	ID	TRBV	CDR3β SEQUENCE	TRBJ	FREQUENCY (%)
A22Cα$^{-/-}$	10F11	19	CASSIRTGGAETLY	2-3	100
	10F12	19	CASSMRQGGAETLY	2-3	100
	30B6	19	CASSIRQGGAETLY	2-3	94.74
		19	CASSIRQGDAETLY	2-3	5.26
	30C4	19	CASSMRQGGAETLY	2-3	88.89
		19	CASSRRDRGAETLY	2-3	11.11
	30D7	19	CASSSGLEQY	2-7	93.75
		19	CASSFREEGAETLY	2-3	6.25
	30F7	19	CASSIRTGGAETLY	2-3	94.12
		24	CASSRDSDTEVF	1-1	5.88
A22Cα$^{-/-}$*PI2*$^{-/-}$	1F9	19	CASSIRQGGAETLY	2-3	96
		19	CASSFREEGAETLY	2-3	4
	30A6	19	CASSFREEGAETLY	2-3	100
	30B9	19	CASSMRQGGAETLY	2-3	69.23
		19	CASSFREEGAETLY	2-3	23.08
		19	CASSIREGGAETLY	2-3	7.69
	30D4	19	CASSIRQGGAETLY	2-3	94.12
		19	CASSVRQGGAETLY	2-3	5.88
	30D8	19	CASSFREEGAETLY	2-3	50
		19	CASSIRQGGAETLY	2-3	25
		19	CASSFRQEGAETLY	2-3	16.67
		19	CASSMRQRGAETLY	2-3	8.33
	30H3	19	CASSIRQGGAETLY	2-3	100
A22Cα$^{-/-}$*PI1*$^{-/-}$ *PI2*$^{-/-}$*Y16A*^{tg}	1G3	19	CASSMRQGGAETLY	2-3	100
	3F11	19	CASSMRQGGAETLY	2-3	63.64
		19	CASSRRDRGAETLY	2-3	31.82
		4	CASSQDGQDTQY	2-5	4.55
	3G5	19	CASSIRQGGAETLY	2-3	100
	10G2	19	CASSMRQGGAETLY	2-3	58.33
		19	CASSFREEGAETLY	2-3	33.33
		19	CASSFRQEGAETLY	2-3	8.33
	30A8	19	CASSMRQGGAETLY	2-3	100
	30B8	19	CASSMRQGGAETLY	2-3	100
	30E2	19	CASSIRTGGAETLY	2-3	61.9
		19	CASSMRQGGAETLY	2-3	33.33
		19	CASSFREEGAETLY	2-3	4.76
	30H1	19	CASSIRQGGAETLY	2-3	100

Table 2: CDR3β sequences of insulin B15-23-reactive oligoclonal lines. Colored sequences represent those found in more than one mouse. Non-germline-encoded motifs are underlined in bold.

Figure Legends

Figure 1. $CD4^+$ and $CD8^+$ T cell numbers in the thymus are unaffected by proinsulin expression

Live single-positive $CD4^+$ and $CD8^+$ T cells were quantified in single cell suspensions of thymus from mice aged 4-7 or 12-16 weeks. Representative flow cytometry plots (**A**), total $CD4^+$ T cell numbers (**B**), and total $CD8^+$ T cell numbers (**C**) are displayed for all strains. Data are shown for 9-12 mice per group (encompassing 3-4 experiments). Males and females were included as no differences were detected when analyzed separately. Significance was assigned at $p<0.01$ (**).

Figure 2. Proinsulin-specific and age-related effects on TRBV19 expression

$CD8^+$ T cells expressing TCRVβ6 (TRBV19) were quantified in single cell suspensions of thymus (**A**, **B**) and pancreatic lymph nodes (PLN) (**C**, **D**) from mice aged 4-7 (**A**, **C**) or 12-16 (**B**, **D**) weeks. Data are shown for 9-12 mice per group (encompassing 3-4 experiments). Males and females were included as no differences were detected when analyzed separately. Significance was assigned at $p<0.05$ (*) and $p<0.01$ (**).

Figure 3. PI2 deficiency increases the proportion of insulin B15-23-reactive $CD8^+$ T cells

H-$2K^d$-LYLVCGERG $tetramer^+CD8^+$ T cells were quantified in single cell suspensions of thymus, spleen, pancreatic lymph nodes (PLN), and mesenteric lymph nodes (MLN) from mice aged 4-8 weeks. Non-specific staining was quantified using the minimal H-$2K^d$-AYAAAAAAV tetramer. Data are shown after background subtraction for 5-10 mice per group. Males and females were included as no differences were detected when analyzed separately. Significance was assigned at $p<0.05$ (*) and $p<0.01$ (**).

Figure 4. Mice deficient in PI2 develop spontaneous diabetes

Mice were housed together from weaning and tested weekly for glycosuria using Diastix. Positive results were validated 24 hours later, and diabetes was confirmed by a blood glucose level >13.9mmol/l. Only males were included as no females developed diabetes. Significance was assigned at $p<0.05$ (*).

Figure 5. The TCRVβ repertoire of insulin B15-23-reactive $CD8^+$ T cells

H-$2K^d$-LYLVCGERG $tetramer^+CD8^+$ T cells were sorted by flow cytometry from single cell suspensions of pancreatic lymph nodes (PLN) from mice aged 4-8 weeks and analyzed for *TRB* gene expression using an unbiased molecular approach. Data are shown for 5-7 mice per group, comprising a total of 6-20 distinct clonotypes.

Figure 6. $TRBV19^+CD8^+$ T cells exhibit low levels of functional sensitivity to insulin B15-23

Oligoclonal $TRBV19^+CD8^+$ T cell lines expanded in the presence of insulin B15-23 were analyzed for cytotoxic activity (**A**), MIP1β (**B**), and IFNγ (**C**) production. Data are shown for representative clones (*A22Cα*$^{-/-}$: 10F12; *A22Cα*$^{-/-}$*PI2*$^{-/-}$: 30A6; *A22Cα*$^{-/-}$*PI1*$^{-/-}$*PI2*$^{-/-}$*Y16A*^{tg}: 1G3).

Figure 1

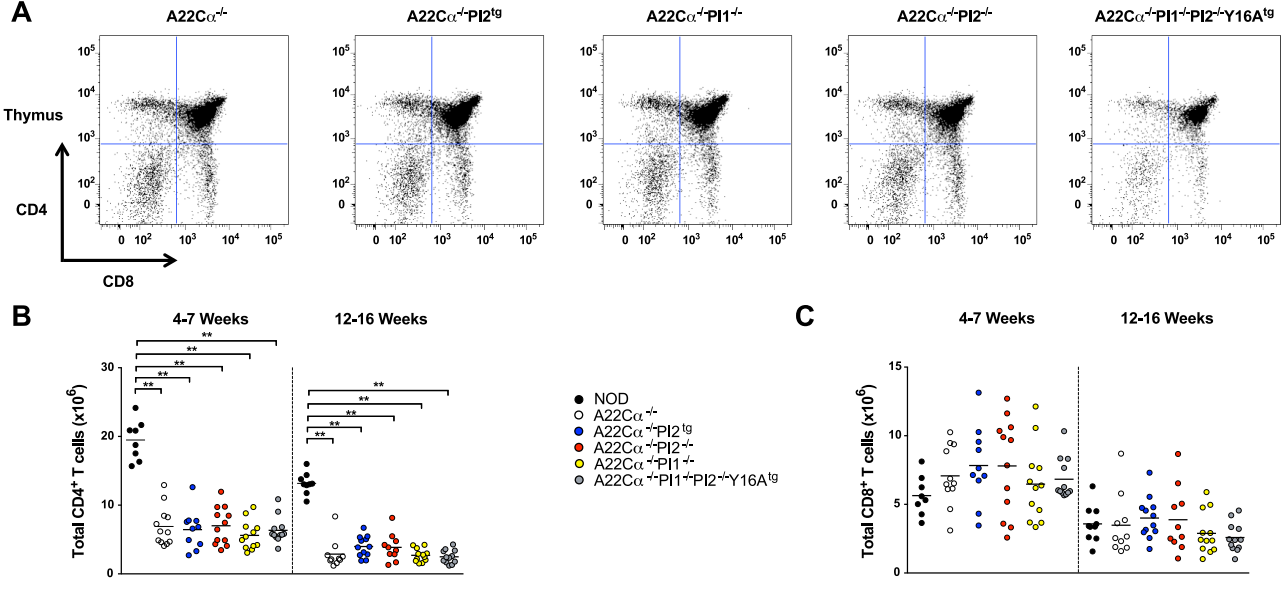
A
A22Cα-/-
A22Cα-/-PI2tg
A22Cα-/-PI1-/-
A22Cα-/-PI2-/-
A22Cα-/-PI1-/-PI2-/-Y16Atg
Thymus
CD4
CD8
B
4-7 Weeks
12-16 Weeks
Total CD4+ T cells (x10^6)
NOD
A22Cα-/-
A22Cα-/-PI2tg
A22Cα-/-PI2-/-
A22Cα-/-PI1-/-
A22Cα-/-PI1-/-PI2-/-Y16Atg
C
4-7 Weeks
12-16 Weeks
Total CD8+ T cells (x10^6)

Figure 2

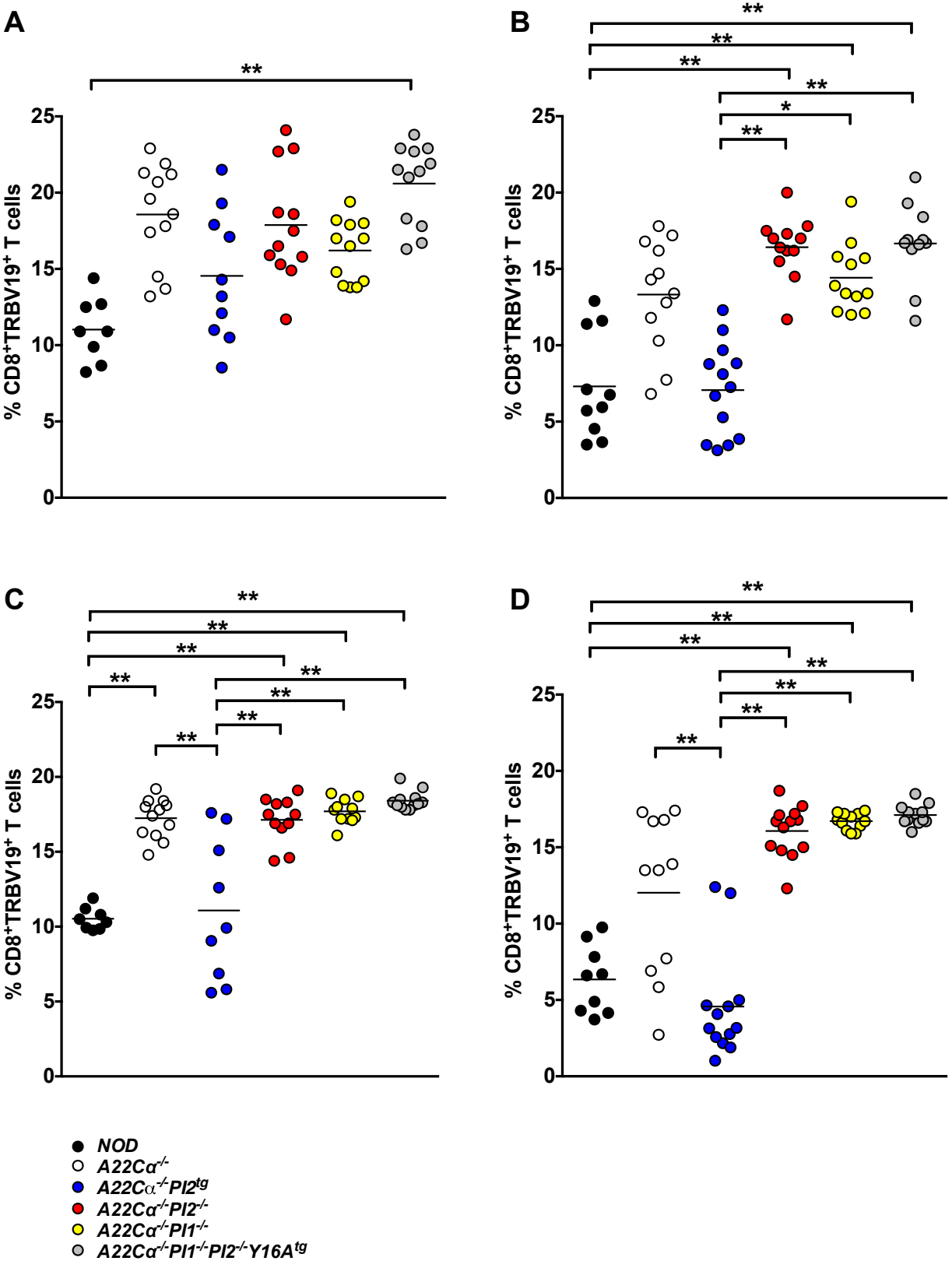
A
B
C
D
% CD8+TRBV19+ T cells
0
5
10
15
20
25
**
*
NOD
A22Cα-/-
A22Cα-/-PI2tg
A22Cα-/-PI2-/-
A22Cα-/-PI1-/-
A22Cα-/-PI1-/-PI2-/-Y16Atg

Figure 4

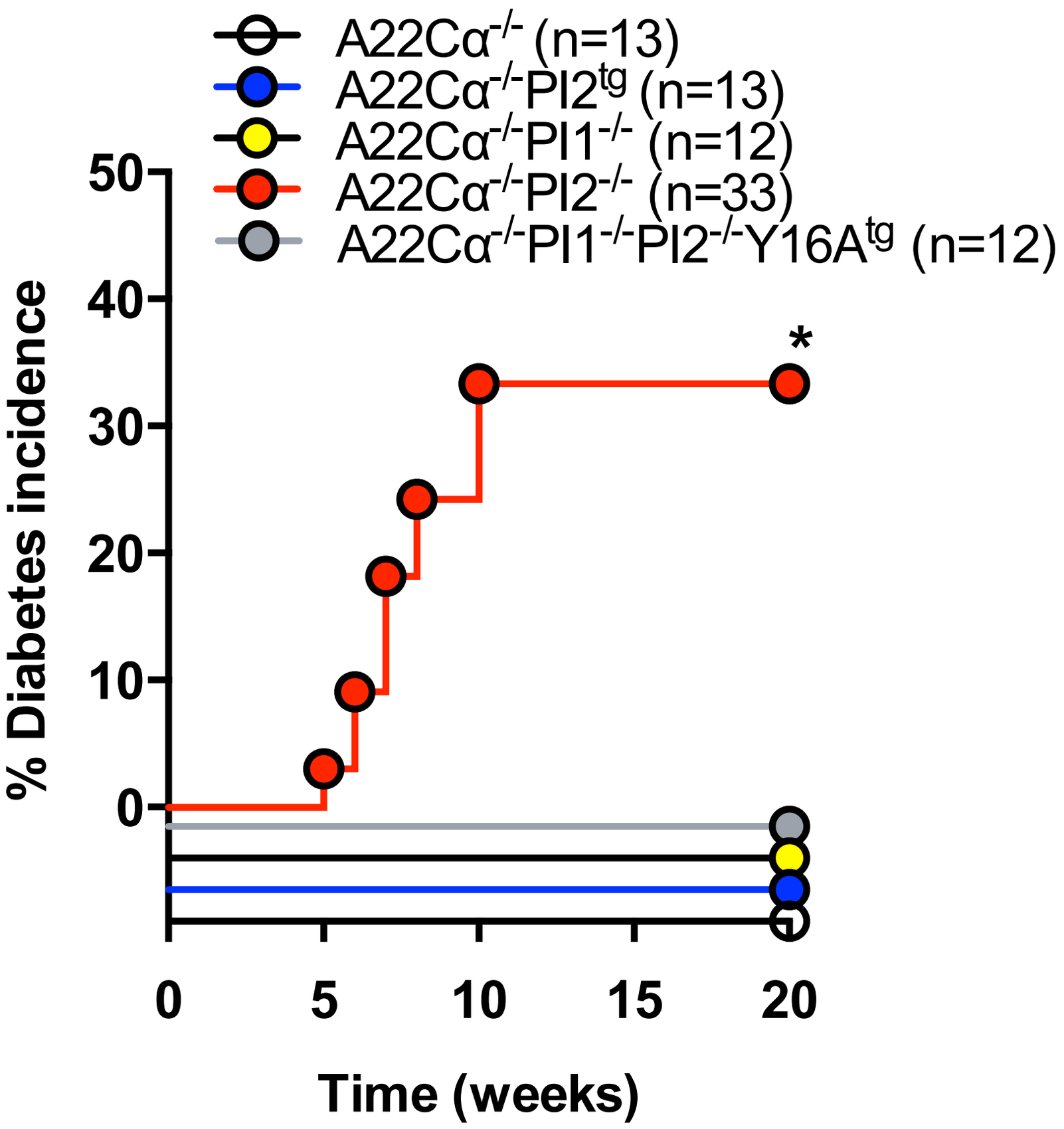
A22Cα-/- (n=13)
A22Cα-/-PI2tg (n=13)
A22Cα-/-PI1-/- (n=12)
A22Cα-/-PI2-/- (n=33)
A22Cα-/-PI1-/-PI2-/-Y16Atg (n=12)
% Diabetes incidence
50
40
30
20
10
0
*
0
5
10
15
20
Time (weeks)

Figure 3

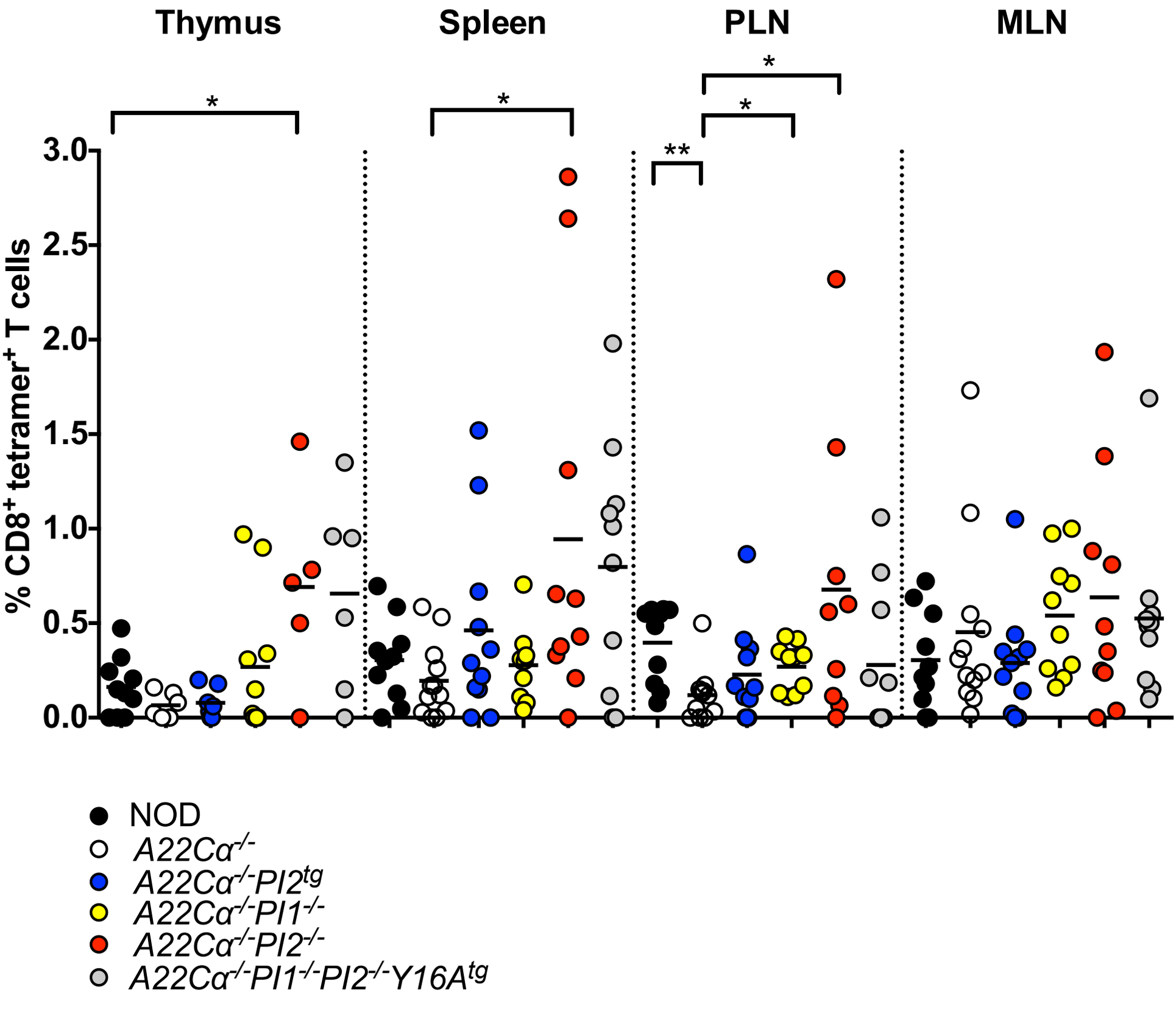
Thymus
Spleen
PLN
MLN
*
*
*
*
**
3.0
2.5
2.0
1.5
1.0
0.5
0.0
% CD8+ tetramer+ T cells
NOD
A22Cα-/-
A22Cα-/-PI2tg
A22Cα-/-PI1-/-
A22Cα-/-PI2-/-
A22Cα-/-PI1-/-PI2-/-Y16Atg

Figure 5

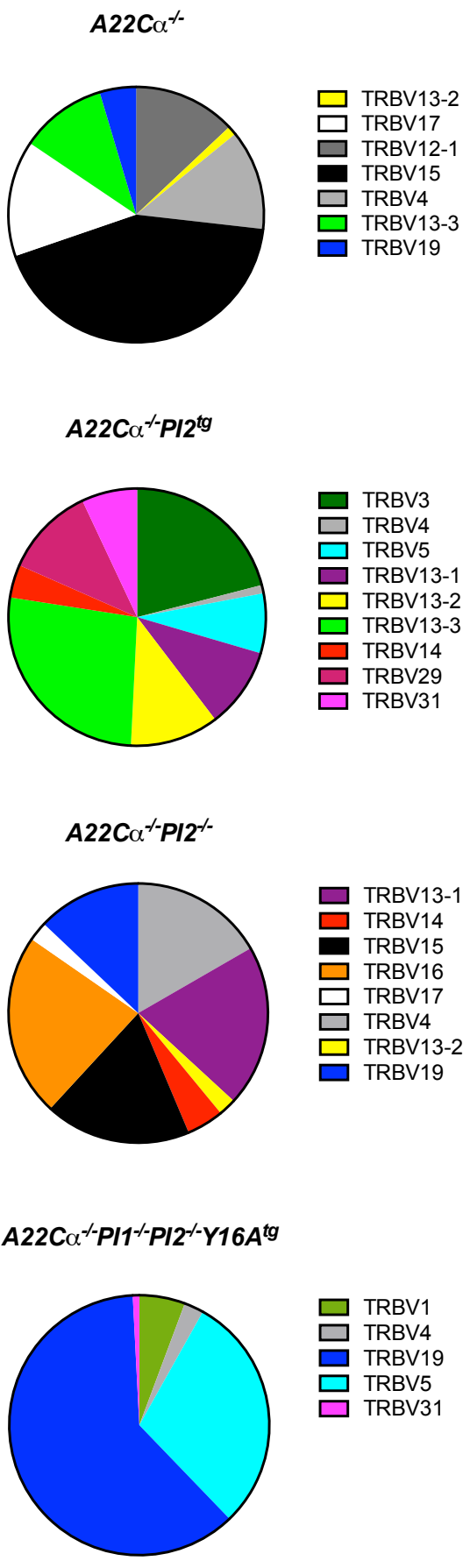
A22Cα-/-
TRBV13-2
TRBV17
TRBV12-1
TRBV15
TRBV4
TRBV13-3
TRBV19
A22Cα-/-PI2tg
TRBV3
TRBV4
TRBV5
TRBV13-1
TRBV13-2
TRBV13-3
TRBV14
TRBV29
TRBV31
A22Cα-/-PI2-/-
TRBV13-1
TRBV14
TRBV15
TRBV16
TRBV17
TRBV4
TRBV13-2
TRBV19
A22Cα-/-PI1-/-PI2-/-Y16Atg
TRBV1
TRBV4
TRBV19
TRBV5
TRBV31

Figure 6

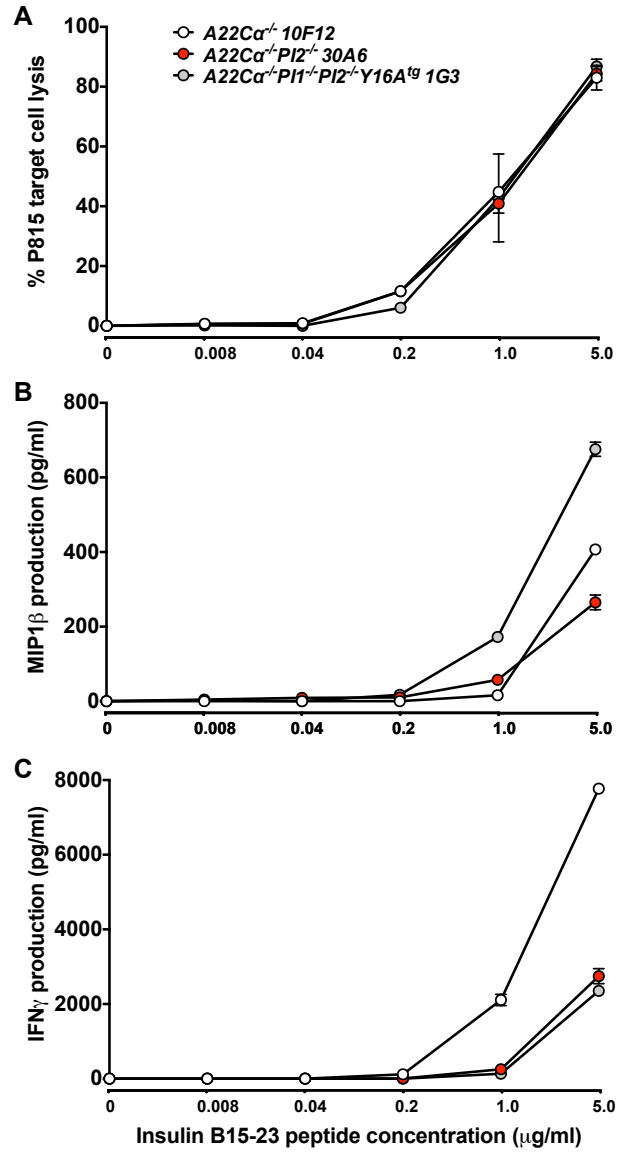
A
% P815 target cell lysis
A22Cα-/- 10F12
A22Cα-/-PI2-/- 30A6
A22Cα-/-PI1-/-PI2-/-Y16Atg 1G3
B
MIP1β production (pg/ml)
C
IFNγ production (pg/ml)
Insulin B15-23 peptide concentration (μg/ml)

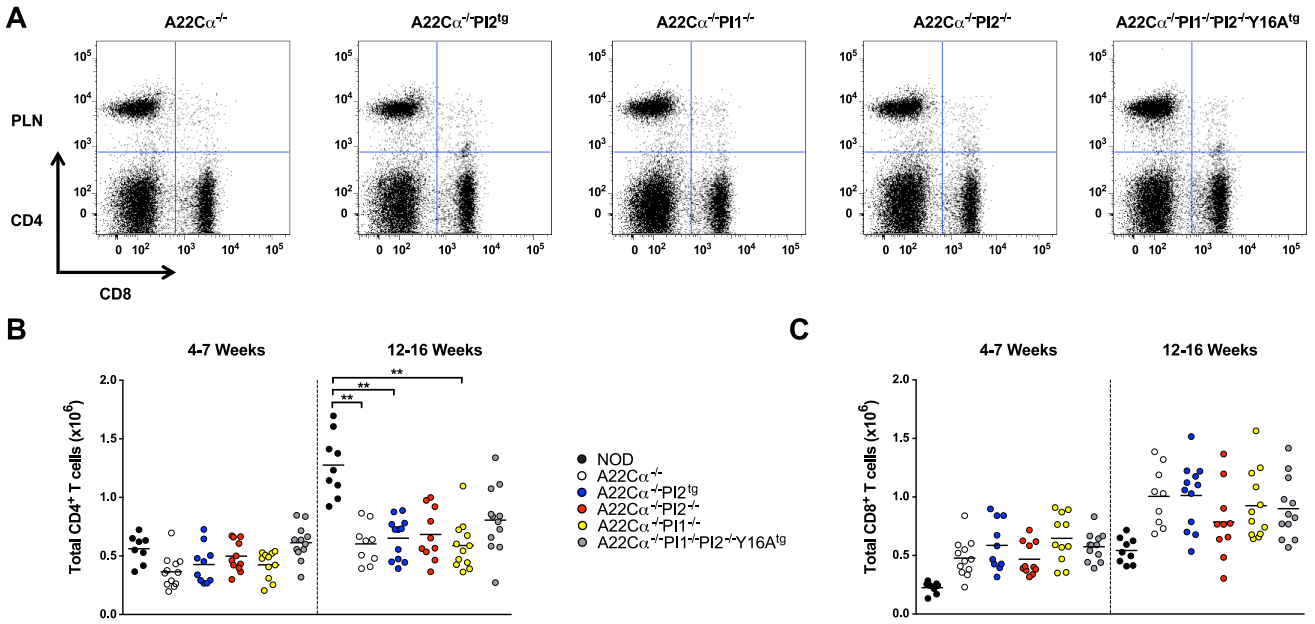

SUPPLEMENTAL FIGURE 1: **CD4⁺ and CD8⁺ T cell numbers in the periphery are unaffected by proinsulin expression.** Live single-positive CD4⁺ and CD8⁺ T cells were quantified in single cell suspensions of pancreatic lymph nodes (PLN) from mice aged 4-7 or 12-16 weeks. Representative flow cytometry plots (**A**), total CD4⁺ T cell numbers (**B**), and total CD8⁺ T cell numbers (**C**) are displayed for all strains. Data are shown for 9-12 mice per group (encompassing 3-4 experiments). Males and females were included as no differences were detected when analyzed separately. There were no significant differences between groups.

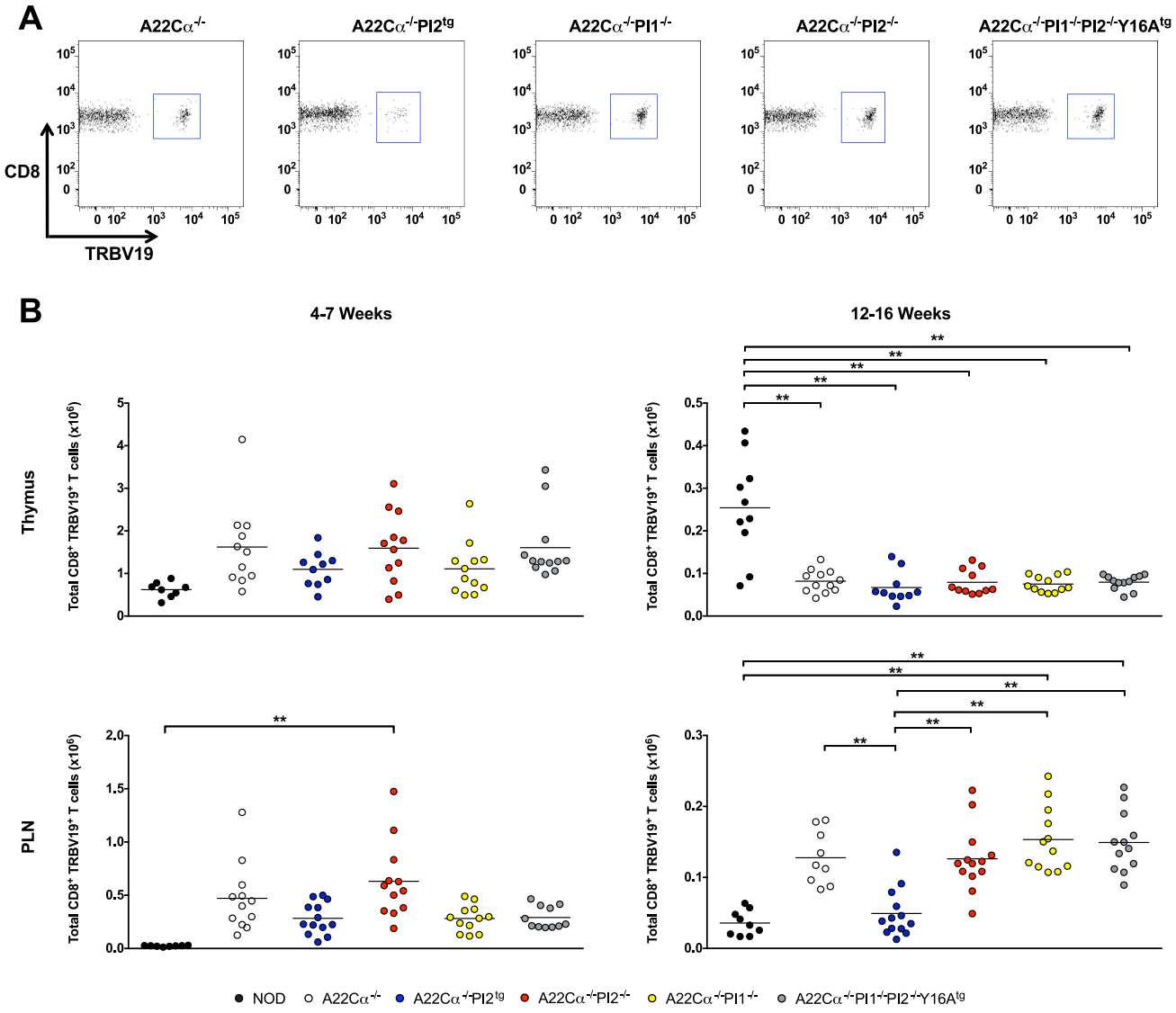

SUPPLEMENTAL FIGURE 2: **Proinsulin-specific and age-related effects on TRBV19 expression.** CD8$^+$ T cells expressing TCRVβ6 (TRBV19) were quantified in single cell suspensions of thymus and pancreatic lymph nodes (PLN) from mice aged 4-7 or 12-16 weeks. Representative flow cytometry plots (PLN from mice aged 12-16 weeks) (**A**) and total TRBV19$^+$CD8$^+$ T cell numbers (**B**) in the thymus (top row) and PLN (bottom row) are displayed for all strains. Data are shown for 9-12 mice per group (encompassing 3-4 experiments). Males and females were included as no differences were detected when analyzed separately. Significance was assigned at $p<0.01$ (**).

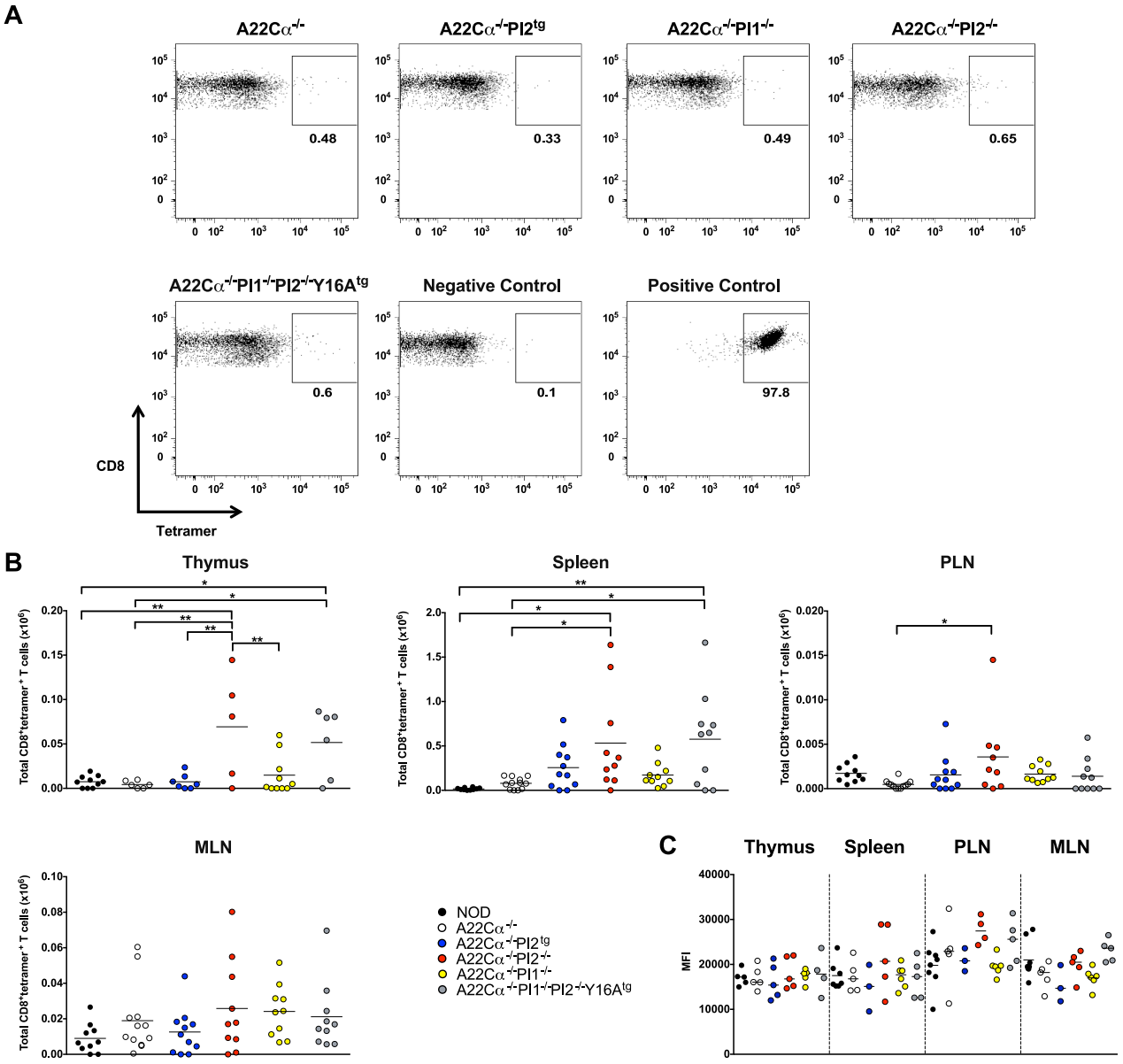

SUPPLEMENTAL FIGURE 3: **PI2 deficiency increases the number of insulin B15-23-reactive CD8⁺ T cells.** H-2K^{d}-LYLVCGERG tetramer^{+}CD8^{+} T cells were quantified in single cell suspensions of thymus, spleen, pancreatic lymph nodes (PLN), and mesenteric lymph nodes (MLN) from mice aged 4-8 weeks. Representative flow cytometry plots, including positive (G9C8 transgenic mice) and negative (H-2K^{d}-AYAAAAAAV tetramer) controls (**A**), total tetramer^{+}CD8^{+} T cell numbers (**B**), and mean fluorescence intensity (MFI) values (**C**) are displayed for all strains. Data are shown for 5-10 (**B**) or 3-8 (**C**) mice per group. Males and females were included as no differences were detected when analyzed separately. Significance was assigned at $p<0.05$ (*) and $p<0.01$ (**).

SUPPLEMENTAL TABLE 1: **Insulitis scores in non-diabetic mice at 20 weeks of age.**

Strain	**Insulitis score**			
	0	**1**	**2**	**3**
A22Cα$^{-/-}$	75.3%	12.7%	12%	0
A22Cα$^{-/-}$*PI2*$^{-/-}$	76.7%	11.9%	11.9%	2.0%
A22Cα$^{-/-}$*PI1*$^{-/-}$*PI2*$^{-/-}$ *Y16A*^{tg}	100%	0	0	0

Insulitis scores are shown for 96-144 islets from 3-7 mice per group. The following criteria were used: 0, no insulitis, 1, peri-insulitis, 2, <50% of islet infiltrated 3, >50% of islet infiltrated.

SUPPLEMENTAL TABLE 2: **CDR3β sequences of insulin B15-23-reactive CD8$^+$ T cells**

Strain	CDR3β sequence	Freq. (%)
A22Cα$^{-/-}$	CASSLGGYEQY	35.16
	CASGDWGGYQDTQY	1.15
	CASSFILGGYAEQF	12.68
	CASSDYGDANTEVF	5.48
	CASTRHHTEVF	4.61
	CASTGNTGQLY	0.58
	CASSQDRSNTEVF	7.20
	CASSRVPGEQY	14.12
	CASSRAPGEQY	0.29
	CAGSRVPGEQY	0.29
	CASLVETLY	12.68
	CASSDAWAGGQDTQY	5.48
	CASLAETLY	0.29
A22Cα$^{-/-}$PI2^{tg}	CASRRDIYNSPLY	91.71
	CASGPGTGGFTEVF	6.08
	CASSRDIYNSPLY	2.21
A22Cα$^{-/-}$PI2$^{-/-}$	CASSIRESGAETLY	12.94
	CASSRDNTEVF	2.41
	CASSLVSQDTQY	2.19
	CASGDAVEQY	2.19
	CASSHRGNTEVF	15.57
	CVSSHRGNTEVF	0.88
	CASSHRGNTEAF	0.22
	CASSEGQGGDTQY	17.54
	CAGSEGQGGDTQY	0.22
	CASSLGGYEQY	13.60
	CASSLGGYGQY	4.61
	CASRSGGTGNTLY	2.19
	CASRSGGPGNTLY	0.22
	CASSLDRNQNTLY	20.61
	CASSYRGPNQDTQY	4.61
A22Cα$^{-/-}$PI1$^{-/-}$PI2$^{-/-}$Y16A^{tg}	CASSPAGSTLY	28.46
	CASSLTGNTGQLY	2.44
	CASSGDYAEQF	32.93
	CAWSLAGGGQY	0.81
	CASSPDNYEQY	29.67
	CTCSADYAEQF	5.69

Colored sequences represent those found in more than one mouse.